HIGH QUALITY PV-GRID SYSTEM INTEGRATION INCLUDING VSC REACTIVE POWER SUPPORT

A.Samir
Faculty of Engineering
Cairo University
Cairo, Egypt
Ammar_samir21@yahoo.com

M.Taha
Faculty of Engineering
Cairo University
Cairo, Egypt
mohamd.taha@cu.edu.eg

M. Muhammad sayed
Faculty of Engineering
Cairo University
Cairo, Egypt
fecu.msayed@gmail.com

A. Ibrahim
Faculty of Engineering
Cairo University
Cairo, Egypt
drahmedibr@gmail.com

Abstract: *In this work, a complete model for the integration between the Photovoltaic Distributed Generation System (PV-DGS) and the utility grid has been modeled and simulated by MATLAB/SIMULINK. The aims of this study are support the active power to a given feeder, and improvement the output power quality from the PV-DGS unit. Two PV-arrays with total power yield equal to 200KW have been modeled. The maximum power point tracking based on the perturb and observe technique has been used to control the DC-DC converter. The voltage source converter using the space vector modulation has been modeled in the DQ frame to allow the system to operate in different modes. These modes are the unity output power factor and the reactive power compensation .Different control techniques have been applied including the conventional PI controller as well as the intelligent optimization tuning. A complete comparison between both techniques has been introduced and analyzed.*

Key words: *DGS, GA, PV, SVM, and VSC.*

1. INTRODUCTION

The new techniques for increasing the production of electricity based on the renewable energy sources like wind, solar Photovoltaic (PV) and tidal energy should be encouraged .These new strategies must be able to overcome to the significant and regular rise in load demand, the growing concerns about environmental pollution and the fast reduction of conventional resources challenges [1- 3].Among the renewable energy resources, the solar PV is the most essential and primary sustainable resource because its availability in abundance in the most world countries. The goal of this study is to reach to a high quality connection between the Photovoltaic Distributed Generation System (PV-DGS) and a given feeder. So, besides pumping the active power to the utility grid, this study focuses on the quality of the output power from the PV-DGS. One of the drawbacks in connecting the PV-DGS to the utility grid is the voltage variation at the point of common coupling (PCC). The voltage variation results from the variation in the solar radiation and the conventional control methods for the PV-inverter [3]. The voltage profile of the PV-DGS determines the maximum PV-DGS at a given feeder. The aim of DGS is not only generate an active power to the utility grid but also support many auxiliary activities (e.g. power factor correction, dynamic stability, reactive power support, etc.)[3]. Injecting reactive power has a role to play for improving the PCC-voltage profile, the grid power quality, reducing the transmission losses and finally, facing loads that have complex and unpredictable nature like the reactive or industrial loads. More works have been made to solve the issues related to the maximum PV-DGS penetration [3].Some authors [4- 6] have focused to present a solution for mitigating the instability voltage by setting up energy storages at either the user end or the load

dispatch center. Unfortunately, this solution isn't economically and practically [3]. Rueda-Media et al. [7] have focused on the ancillary activities in the DGS units like the reactive power support to enhance the PV-DGS penetration. Steffel et al. [8] have highlighted the importance of using a centralized volt-var control by the service provider that mitigates the over-voltage (OV) issue and enhance the PV-DGS penetration. A number of other authors [9, 10] have suggested forcing the PV-grid inverter to compensate a reactive power that helps in mitigating voltage variation. Rupesh G. Wandhare et al. [3] have proposed a system combines between distribution static synchronous compensator (D-STATCOM) and the PV inverter for compensation duty. This proposed system has an auxiliary converter to overcome on the transient issues that result from inadequacy of PV-DGS output voltage and the D-STATCOM voltages. This paper presents an analysis and simulation of PV-DGS connected to the utility grid. The high quality of the system output power has been done by forcing VSC to compensate reactive power with 20KVAR capacitor bank. An intelligent optimization technique has been used for improving the controller performance and the entire system efficiency. A complete comparison between operating the VSC in unity power factor mode and in reactive power compensating mode has been introduced and analyzed.

2. PV-DGS COMPONENTS

This section introduces the various important parts of the PV-DGS that is illustrated in Fig.1.The main components are the PV-array, DC-DC converter including the maximum power point tracking (MPPT) algorithm, Energy storage capacitors, The voltage source converter (VSC) including the space vector modulation (SVM) as switching technique and its feedback control unit, Electrical isolated transformer, and three phases - controlled breaker. The power electronic converters have been used to overcome on the intermittent issue. They have been used to regulate voltage, frequency, and power output characteristics [11].The DC-output voltage is regulated by the DC-DC converter to be used as the fixed input DC-voltage for VSC. The MPPT algorithm calculates the optimal duty cycle (D) to continuously confirm that the PV-DGS operates at the maximum power point (MPP). Energy storage capacitors have been used to smooth the power that is generated from the PV-array and to balance the difference between the average and instantaneous power [12]. The PV-DGS has used three phase two- level VSC' MOSFET/Diodes' as a DC to AC converter .Its function is to transform DC input voltage to asymmetric AC output voltage with desired magnitude and frequency [12, 13].The VSC has three control loops that can be defined as active power controller or V_{DC} regulator, reactive power controller and The inner loops or the Current regulators that produce the controlled voltage signal to SVM. SVM helps to match the VSC output with the utility grid. The VSC controllers use both conventional and intelligent tuning for parameter tuning process**.** The VSC is the main element in the PV-DGS. The VSC has many details that are related to its structure, modulation technique and control unit. In the following section, The VSC will be described in more details.

3. THE GRID VSC SYSTEM: CONTROL IN DQ-FRAME

In this section, the different components of the VSC will be introduced. The Free-wheeling diode is necessary to give a path for release the energy that is stored in the inductor when Voltage drops to zero [12, 14]. The connection between the VSC and the utility grid is done by using a harmonic "grid" Filter [R+L]. The aim of the harmonic filter is to attenuate the output voltage harmonics of the VSC [12]. The Step up transformer has been used for the electrical isolation between PV-DGS and Utility grid [15, 16].In the current mode control, both power components are controlled by the VSC line current with respect to the PCC voltage [14].The VSC line current is regulated by a current-regulation loop and it can define as the inner control loop of the VSC [14].

In this study, V_{DC} and the PI controller have been used to regulate the DC-power port. The tuning parameter of PI controller is determined by both auto tuning tool and GA-optimization technique in the MATLAB/SIMULINK. The cycle of DC voltage control technique start with that the measured V_{DC} is compared with V_{DCref} and the result error signal is treated by the PI-Controller and the controller output I_{dref} is used for the inner control loop as a reference variable in the real - power term. The inner control loop work to regulate I_d at I_{dref} [3, 14].The transferred Reactive power Q_s can be separately controlled. In several applications, Q_s is regulated at zero, which means the PV-DGS operates in unity power factor mode. Otherwise, Q_s can be controlled by using a closed-loop mechanism to adjust the PCC- voltage. The two modes of Qs controller are illustrated in this study [14, 17].

Sections (4.4), (4.5) and (4.6) in [14] presented the space phasor expressions for the instantaneous power components in terms of dq-frame variables. So, the power components expressions that transferred to the AC-utility grid at PCC are

$$p = \frac{2}{3}\left[u_d\, i_d + u_q i_q\right], \quad (1)$$

$$q = \frac{2}{3}\left[u_q\, i_d - u_d i_q\right]. \quad (2)$$

Where(u_d , u_q) are defined as the transformed grid voltages components in terms of dq-frame and (i_d, i_q) are the current components in terms of dq-frame. If the synchronous frame is aligned to voltage, the quadrature composite of the grid voltages will be equal zero. Therefore, the power equations reduce to

$$p = \frac{2}{3}\left[u_d\, i_d\right], \quad (3)$$

$$q = -\frac{2}{3}\left[u_d i_q\right]. \quad (4)$$

Equation (3) and Equation (4) proved that the independent control of the power components is done by controlling the VSC dq current components (i_d , i_q) [14]. The governing circuit equations for the current controller design will be defined in synchronously rotating reference frame. Section (8.3.2) in [14] presented the representation of space phasors in dq-frame and section (8.3.3) in [14] focused on the dynamic model of the power components controller .The equations of the dynamic model are

$$L\frac{di_d}{dt} = Lw(t)i_q - (R + r_{on})i_d + V_{td} - \widehat{V_s}\cos(w_0 + \theta_0 + p), \quad (5)$$

$$L\frac{di_q}{dt} = -Lw(t)i_d - (R + r_{on})i_q + V_{tq} - V_s\sin(w_0 + \theta_0 - p). \quad (6)$$

Where $\widehat{V_s}$ is the maximum value of the phase voltage,w_0 is the utility grid frequency, θ_0 is the initial phase angle, and p is the phase shift. By assuming the steady state condition and substituting for $w(t) = w_0$ and $p = w_0 + \theta_0$ [3, 19].we deduce

$$L\frac{di_d}{dt} = Lw_0 i_q - (R + r_{on})i_d + V_{td} - V_{sd}, \quad (7)$$

$$L\frac{di_q}{dt} = -Lw_0 i_d - (R + r_{on})i_q + V_{tq} - V_{sq}. \quad (8)$$

Equation (7) and Equation (8) illustrate two decoupled second-order linear systems. Where V_{sd} , V_{sq} are the grid voltage components in terms of dq-frame; i_d , i_q are the direct and quadrature current components; L and R are the harmonic filter. V_{td} , V_{tq} are the input voltage signal to SVM unit [18 ,19]. i_d and i_q are state variables, V_{td} and V_{tq} are control inputs and the grid voltage components V_{sd} , V_{sq} are feed -forward compensation [3]. Taking into consideration that the Voltage vector is set at d-axis, so $V_{sq} \cong 0$ .The VSC input voltage must be constant , So the variable DC-power source with regulation control mechanism has be used or assuming large C_{DC} has be used [3]. This assumption renders (7) and (8) as the first order linear system and by defining new variables U_d and U_q[14];

$$U_d = L\frac{di_d}{dt} + (R + r_{on})i_d, \quad (9)$$

$$U_q = L\frac{di_q}{dt} + (R + r_{on})i_q. \quad (10)$$

The Laplace transfer is operated on (9) and (10) and the modification form is shown below

$$U_d(s) = L\,S\,i_d(s) + (R + ronid(s)), \quad (11)$$

$$U_q(s) = LS\,i_q(s) + (R + roniq(s)). \quad (12)$$

The next transfer function can be used for the VSC current loops;

$$\frac{I_d(s)}{U_d(s)} = \frac{I_q(s)}{U_q(s)} = \frac{1}{LS + (R + r_{on})}. \quad (13)$$

Based On (9) and (10), i_d *and* i_q can be controlled by U_d and U_q , respectively.

The closed loop reactive power mechanism has been used to force the VSC to have another function related to exchange reactive power with the utility grid. It became like a static synchronous compensator (STATCOM).In a distribution system, the STATCOM has been used to regulate the voltage [20]. It changes the delivery of the reactive power to the grid. The VSC line current in polar form has been used to control the power components with respect to the voltage of the PCC [14].We exhibit that V_{sabc} can be regulated via the closed loop reactive power mechanism [3, 14].

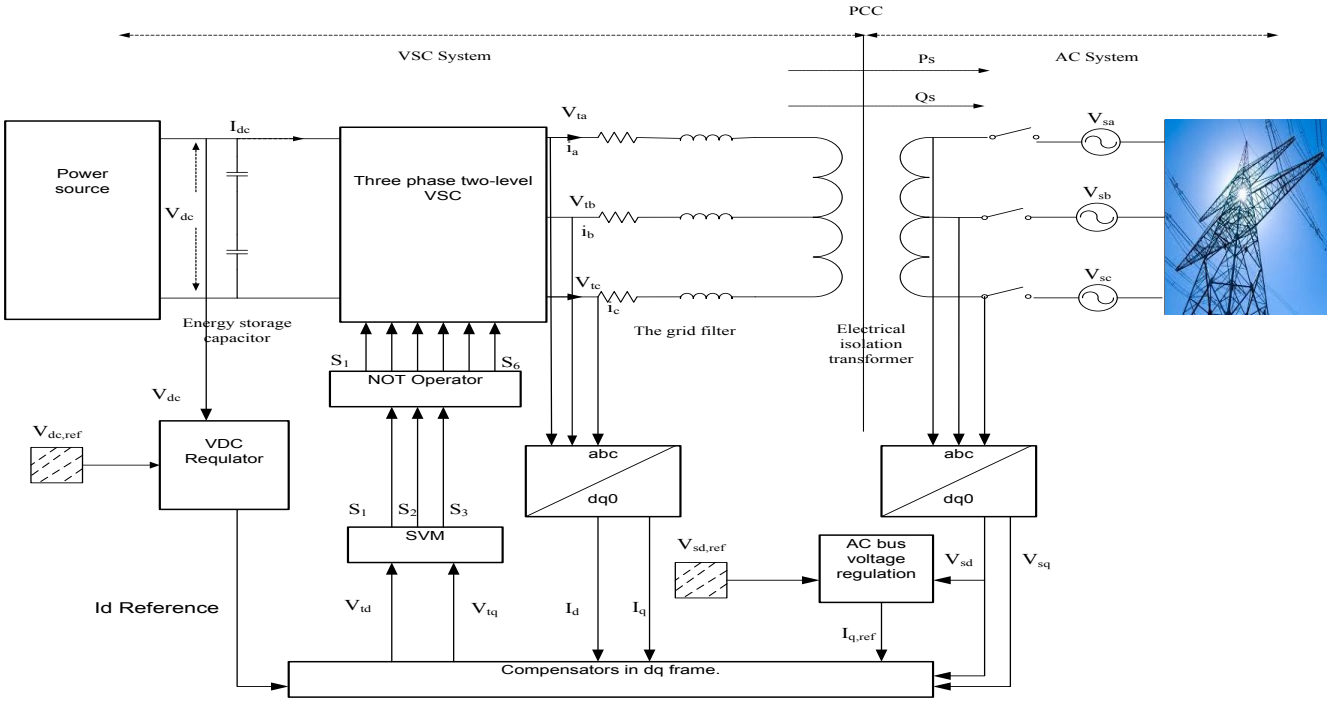

Fig. 1. The main parts of PV-DGS.

4. SPACE VECTOR MODULATION

The normal switching of the VSC causes disconnected positions of the voltage in the Space Vector representation. So, the Space Vector voltage must pursue a circular locus. The required position on this locus can be achieved by an average relationship between two next-door active vectors [21]. The zero state has been used to get a constant interval [22]. The choice of the states and their time duration are done by the space vector (SV) transformation [22].

$$\underline{V_S} \cdot T_s = \underline{V_a} \cdot t_a + \underline{V_b} \cdot t_b + \underline{V_0} \cdot t_0 \ . \quad (14)$$

Where T_s is the sampling period of the given circular locus and t_a , t_b are the time intervals Corresponding to the neighboring vectors V_a , V_b [16, 21].With respect to the sector number, the equations can be written as

$$t_a = \frac{\sqrt{3}}{V_d} \cdot V_s \cdot T_s \cdot \sin\left(\frac{n*\pi}{3} - \alpha\right), \quad (15)$$

$$t_b = \frac{\sqrt{3}}{V_d} \cdot V_s \cdot T_s \cdot \sin\left(\alpha - \frac{n-1*\pi}{3}\right), \quad (16)$$

$$t_0 = T_s - t_a - t_b \ . \quad (17)$$

A. Implementation and advantages of SVM

SVM can be implemented through the next steps that are shown in Fig.3 [16, 21];

1) The output voltage components from the VSC's inner control are converted to the two-phase orthogonal (αβ) plane components.

2) The controlled voltage from last step is transferred to the Phasor form. The Phasor form components are the amplitude (V_s) and the angle (α).

3) The angle (α) from last step have been used to calculate the appropriate sector by compare it to the angles range of each sector.

4) The amplitude (V_s), the angle (α), and the appropriate sector (n) have been used to calculate the time interval (t_a, t_b, t_0) that are shown in (15-17).

5) The switching sequence (01277210) has been used for symmetry reason [16].

5. THE INTELLIGENT OPTIMIZATION TECHNIQUE

The selection process of the PI- Controller parameters to achieve the system performance specification is called the tuning process. There are various conventional methods for PI- controller tuning. Ziegler–Nichols (ZN) method has a set of rules which have been used to set the values of the proportional gain Kp and the integral term K_i .

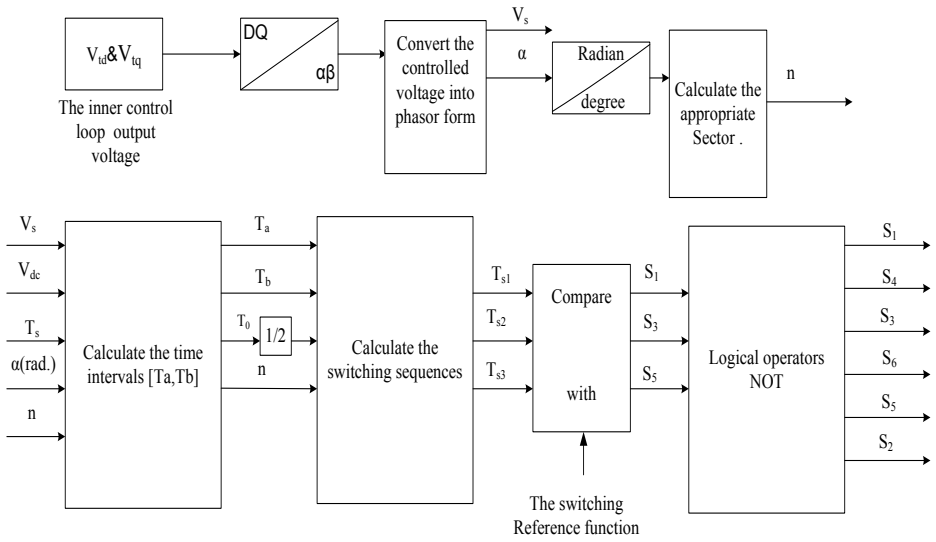

Fig. 2. The SVM implementation block diagram.

The tuning process can depend on the experimental step responses or the value of Kp in case apply the marginal stability when the proportional action only is applied [23]. Conventional method can be improved by integrating optimization techniques. The tuning method based on optimization has design rules related with minimizing certain performance criterion is called performance indices like integral of square error (ISE) or integral of time multiplied by absolute error (ITAE) [24]. In this study, ISE index has been used for quickly eliminating the large errors and a smaller initial overshoot in the resulting response [24]. ISE can be written as

$$\text{ISE} = \int_0^t (e(t))^2. \qquad (18)$$

A. Genetic Algorithms

Genetic Algorithms (GA) is a stochastic optimization technique which is fabricated to mimic the natural selection and the natural biological genetics mechanism. The main concept of GA is based on the survival of the fittest [24], [25]. The mechanism loop of GA begins from creating primary collection of random solutions defined as population. Every individual solution in the random set is defined as a chromosome. The group of chromosomes have been produced from the development process is called the generation. The routine repeating process has been used to produce the Sequential generations which is defined as iterations process. In every repetition, the current chromosomes are estimated by using the problem fitness function. In this study, the performance indices have been used as the fitness function. The next generations are form by either applying the crossover operator or applying the mutation operator [24, 25]. The connection between the GA optimization technique and the given optimization problem is performed by using the MATLAB environment is shown in Fig.4. The goal of this optimization process is minimizing the steady state error by decreasing the ISE performance index .So the GA start searching to the optimum chromosomes that solve the given ISE fitness function. Then the PI-Controller receives the optimum controller parameters and starts output adjustment process to give the desired output.

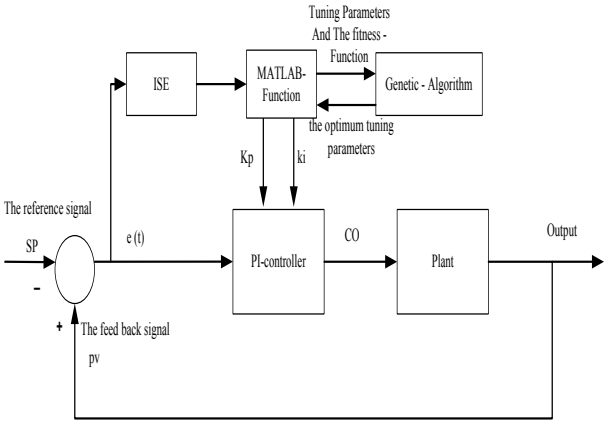

Fig. 3. The block diagram for tuning of PI-Controller parameter using GA.

6. SIMULATION RESULTS AND DISCUSSION

First, the simulation has been performed in the unity power factor mode, so the system can be reduced into two control loops;

1) The outer loop or the voltage regulation loop" V_{DC} Regulator" that produces I_{dref} .

2) The inner loop or the Current regulation that produces the controlled voltage signal or the reference voltage signal to the SVM unit and then the SVM produces the pulse gates for the inverter transistors. Fig.4 shows the simulation result for the PV-DGS without connected load to the low side of transformer. The [PI] controller that is used for controlling the DC- voltage power port is working satisfactorily. That appears in Fig.4 (a) where the measured DC- voltage tracks the reference DC-voltage.the [PI] output signal is the reference current(I_{dref}).

$$e(t) = V_{DCmes} - V_{DCref} . \quad (19)$$

If the error e (t) is positive, i.e. if V_{DCmes} is greater than V_{DCref} , the compensator increasesI_{dref} . That is shown in Fig.5 (a & b).If the error e (t) is negative, i.e. if V_{DCmes} is less than V_{DCref} , the compensator decreasesI_{dref} . I_d And I_q track their references and the optimum value at$V_{DCmes} \cong V_{DCref}$. At this point, the error signal will be zero, and the average power transferred to the utility grid matches the power produced by the PV array as shown in Fig.4 (d). In Fig.4 (c); I_q tracksI_{qref} , and I_{qref} is zero, to maintain the unity power factor. Accordingly, at the steady state, the reactive power that is transferred to the grid equals zero as shown in Fig.4 (e).The 20Kvar static reactive power compensating is connected to the high side voltage of the transformer to help the system to face loads that have complex and unpredictable nature, improve the voltage profile and reduce the transmission losses as shown in Fig.4 (f) [3].

The tuning parameters of the PI controllers are tuned using the intelligent optimization method based on GA .In Table I, the fitness function based on the performance index [ISE] is defined as;

$$\text{The objective function} = x_A \int_0^t (e(t))^2 \, dt + x_B \int_0^t (e(t))^2 + x_C \int_0^t (e(t))^2 . \quad (20)$$

Where x_I is defined as the percentage of presence the ISE of controller I in the final form of the fitness function. In every case, the total ISE in the whole system is estimated. The goal is getting the minimum or optimum value of the total Integral of square error [TISE].Also in the table 1; the optimum tuning parameters of each case are displayed. Table 2 presents the performance of the system in each case and the power components that travel to the utility grid. Static 20 Kvar capacitor bank has been used beside the VSC reactive power share. Also in the table 2, the RMS -phase voltage of the PCC and the voltage waveform total harmonic distortion have been shown. Start with case 1, the fitness function equals zero that means no optimization techniques are applied to the system. The tuning parameters data are taken from Rupesh G. Wandhare et al. [3].The controller B is out of action for reaching to the unity power factor. This unity power factor case has high TISE counts, lower THD and lower tracking PCC-Voltage response to its PCC references voltage. From the data in Table 1 and Table 2, we can infer that case 2 and case5 are the best because they had the lower TISE, the THD in the voltage waveform, the higher active and reactive power travel to the utility grid and the closer PCC-Voltage to the reference voltage. The simulated performance of the PV-System in both case 2 and case5 are shown in Fig.5 and Fig.6.In both figures, it can be noticed that the measured DC-voltage quickly tracks the reference voltage [500V]. This means that the DC-voltage [or the outer] control loop are working satisfactorily. And also the RMS-PCC phase voltage faithfully tracks the reference low side transformer voltage. The VSC share reactive power with static compensator capacitive bank to the utility grid has been observed from both figures. This means that the reactive power mechanism is working satisfactorily. And also can be observed that d-q current component of VSC faithfully track their references. This means that the inner current [or the current regulators] control loops Works properly.

7. CONCLUSIONS

In this study, the PV-DGS and the utility grid has been built and simulated by MATLAB/SIMULINK. The VSC using the SVM has been modeled and analyzed successfully. The feedback control unit of the VSC had been modeled in DQ frame to supply the SVM with accurate controlled voltage signal. The PV-DGS has been simulated in different operating modes. The PV-DGS has been simulated in the unity power factor mode and in the reactive compensation mode. Both conventional PI-Controller parameters tuning and the intelligent optimization tuning were applied to the simulation process. A complete comparison between both modes and tuning techniques has been introduced and analyzed. The final acceptable results confirmed that the high quality connection between the PV-DGS and a given feeder has been achieved when the reactive compensation mode and the intelligent optimization tuning have been applied.

The simulation results showed that besides pumping active power to face the growing loads, the output power quality has been improved. This improvement is achieved by forcing the PV-VSC to compensate reactive power besides 20KVAR reactive capacitors bank. This reactive power mechanism work to progress the system output voltage profile, the minimal voltage variation, and the less THD in the output voltage of the PV-DGS. The simulation results show that the voltage THD is reduced from 0.69% to 0.43% and the phase voltage variation at PCC is reduced from 3.07% to 0.733%.the active power that is generated from PV-DGS is reduced by 0.35%.

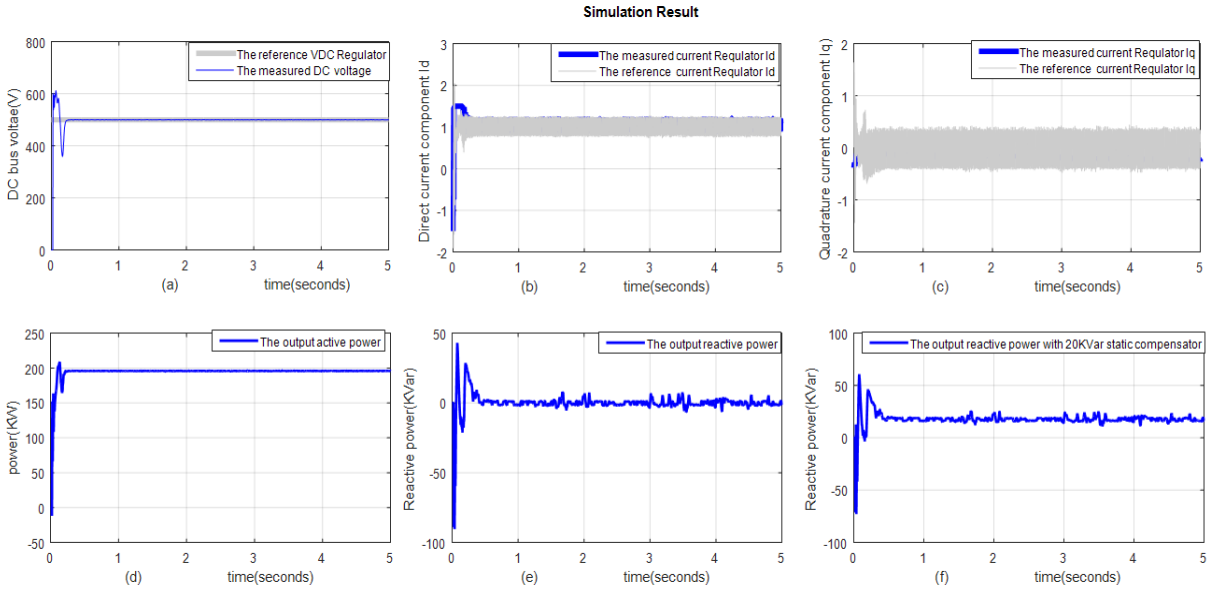

Fig. 4. The simulation result for the system without connected load on low side of transformer. (a) The reference and measured the input DC-voltage for the inverter. (b) The measured and reference direct current component. (c) The measured and reference quadrature current component. (d) The output active power. (e) The output reactive power. (f) The output reactive power including 20kvar as static compensator.

TABLE 1. THE PERFORMANCE INDICES, TISE COUNTS AND THE TUNING PARAMETERS

The different cases Numbers	The fitness-Function define or the performance indices (TISE %)			TISE counts	The tuning parameters					
	Controller A	Controller B	Controller C		Controller A		Controller B		Controller C	
					Kp	Ki	Kp	Ki	Kp	Ki
Case 1	0	0	0	$1.286*10^4$	.014	1.6	-	-	.6283	6.723
Case 2	50	100	100	8077	.02	1.834	2	.862	.319	5
Case 3	100	50	50	8477	.011	1	2.949	.2	.2	5
Case 4	50	50	50	$1.49*10^4$	.0137	1.7202	3.178	.875	.2409	5.912

Case 5	100	100	100	6580	.01	1	2	.404	.368	6

TABLE 2. THE PERFORMANCE OF THE SYSTEM IN DIFFERENT CASES

The different cases Numbers	The RMS-PCC phase voltage			The Active-Power (KW)	The Reactive-Power (Kvar)	THD (%)
	V_A	V_B	V_C			
Case 1	145.2	145.4	145.3	196.17	0	.69
Case 2	148.8	148.9	148.9	195.48	89.32	.51
Case 3	147.2	147.5	147.2	194.78	62.04	.52
Case 4	149.5	149.4	150	194	103.5	.56
Case 5	147.6	147.5	147.6	195.11	62.74	.43

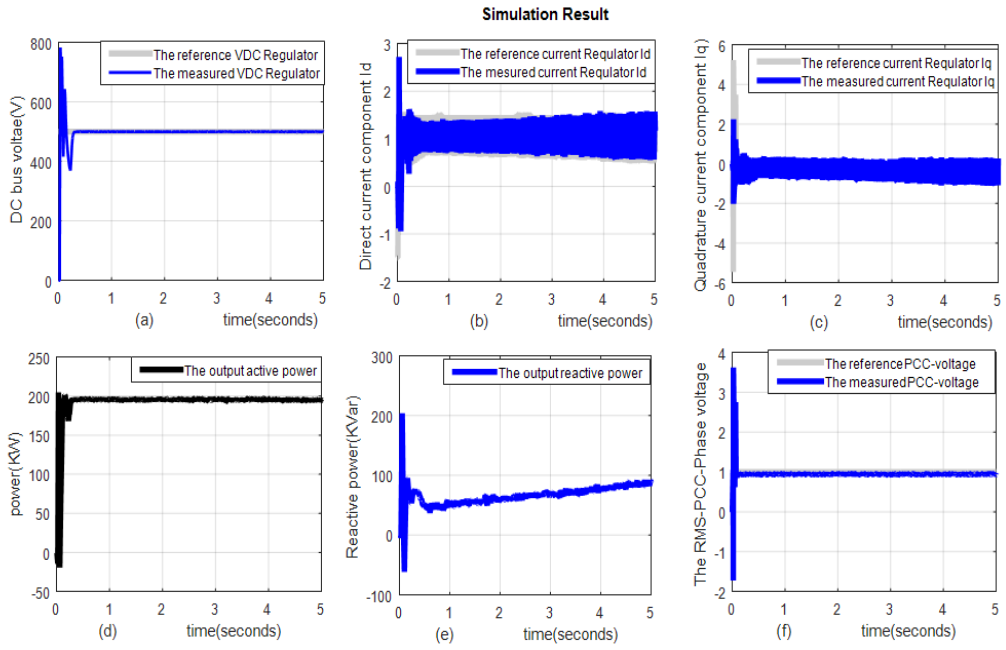

Fig. 5. The simulation result of the PV-System in case2. (a) The reference and measured the input DC-voltage for the inverter. (b) The measured and reference direct current component. (c) The measured and reference quadrature current component. (d) The output active power. (e) The output reactive power. (f) The measured and reference PCC-voltage.

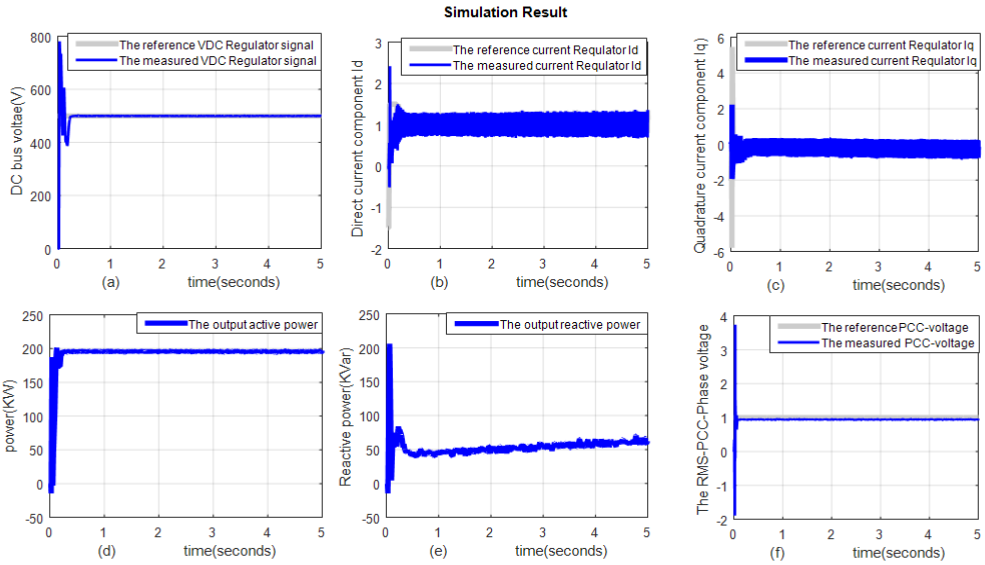

Fig. 6. The simulation result of the PV-System in case5. Figure (a) The reference and measured the input DC-voltage for the inverter. (b) The measured and reference direct current component. (c) The measured and reference quadrature current component. (d) The output active power. (e) The output reactive power. (f) The measured and reference PCC-voltage.

REFERENCES

1. Luiz da Silva, E., Hedgecock, J., Mello, J., Ferreira da Luz, J.: *Practical cost-based approach for the voltage ancillary service*. IEEE Transactions on Power Systems. Vol.16, No.4, 2001, p.806-812.
2. Maloney, M., Mccormick, R., Sauer, R.: *On stranded cost recovery in the deregulation of the U.S. electric power industry*. Nat. Resources J. Stranded Cost Recovery.Vol.37, 1997, p.59-123.
3. Wandhare, R., Agarwal, V.: *Reactive Power Capacity Enhancement of a PV-Grid System to Increase PV Penetration Level in Smart Grid Scenario*. IEEE Transactions on Smart Grid, Vol.5, No.4, 2014, p.1845-1854.
4. Omran, W., Kazerani, M., Salama, M.: *Investigation of Methods for Reduction of Power Fluctuations Generated From Large Grid-Connected Photovoltaic Systems*. IEEE Transactions on Energy Conversion, Vol.26, No.1, 2011, p.318-327.
5. Sugihara, H., Yokoyama, K., Saeki, O., Tsuji, K., Funaki, T.: *Economic and Efficient Voltage Management Using Customer-Owned Energy Storage Systems in a Distribution Network With High Penetration of Photovoltaic Systems*. IEEE Transactions on Power Systems, Vol.28, No.1, p.102-111.
6. Liu, X., Aichhorn, A., Liu, L., Li, H.: *Coordinated Control of Distributed Energy Storage System with Tap Changer Transformers for Voltage Rise Mitigation under High Photovoltaic Penetration*. IEEE Transactions on Smart Grid, Vol.3, No.2, 2012, p.897-906.
7. Rueda-Media, A., Padilha-Feltrin, A.: *Distributed generators as providers of reactive power support-A market approach*. IEEE Trans. Power System, Vol.28, No.1, 2013, p.490-502.
8. Steffel, S., Caroselli, P., Dinkel, A., Liu, J., Sackey, R., Vadhar, N.: *Integrating Solar Generation on the Electric Distribution Grid*. IEEE Transactions on Smart Grid, Vol.3, No.2, 2012, p.878-886.
9. Rogers, K., Klump, R., Khurana, H., Aquino-Lugo, A., Overbye, T.: *An Authenticated Control Framework for Distributed Voltage Support on the Smart Grid. IEEE Transactions on Smart Grid*, Vol.1, No.1, 2010, p.40-47.
10. Di Fazio, A., Fusco, G., Russo, M.: *Decentralized Control of Distributed Generation for Voltage Profile Optimization in Smart Feeders*. IEEE Transactions on Smart Grid, Vol.4, No.3, 2013, p.1586-1596.
11. Chakraborty, S., Simões, M., Kramer, W.: *Power electronics for renewable and distributed energy systems*. 1st Ed.
12. H.Rashid, M.: *Power Electronics Circuits, Devices, and Applications*. 3rd ed., Pearson Prentice Hall, New Jersey, 2004.
13. Mohan, N., Undeland, T., Robbins, W.: *Power electronics*. 1st ed., John Wiley & Sons, Hoboken, New Jersey, 2003.
14. Yazdani, A., Iravani, R.: *Voltage-Sourced Converters in Power Systems*. 1st ed., John Wiley & Sons, Hoboken, New Jersey, 2010.
15. Liserre, M., Blaabjerg, F., Hansen, S.: *Design and Control of an LCL-Filter-Based Three-Phase Active*

Rectifier. IEEE Transactions on Industry Applications, Vol.41, No.5, 2005, p.1281-1291.
16. Abdalrahman, A., Zekry, A., Alshazly, A.: *Simulation and implementation of grid-connected inverters*. International Journal of Computer Applications, Vol.60, No.4, 2012.
17. Yazdani, A., Iravani, R.: *An Accurate Model for the DC-Side Voltage Control of the Neutral Point Diode Clamped Converter*. IEEE Transactions on Power Delivery, Vol.21, No.1, 2006, p.185-193.
18. Schauder, C., Caddy, R.: *Current Control of Voltage-Source Inverters for Fast Four-Quadrant Drive Performance*. IEEE Transactions on Industry Applications, Vol.IA-18, No.2, 1982, p.163-171.
19. Schauder, C., Mehta, H.: *Vector analysis and control of advanced static VAR compensators*. IEEE Proceedings C Generation, Transmission and Distribution, Vol.140, No.4, 1993, p.299.
20. Schauder, C., Gernhardt, M., Stacey, E., Lemak, T., Gyugyi, L., Cease, T. et al.: *Operation of ±100 MVAr TVA STATCON*. IEEE Transactions on Power Delivery, Vol.12, No.4, 1997, p.1805-1811.
21. O. Neacsu, D.: *Space vector modulation – An introduction*. The 27th Annual Conference of the IEEE Industrial Electronics Society, 2001. p. 1583-1592.
22. Kwon, B., Min, B.: *A fully software-controlled PWM rectifier with current link*. IEEE Transactions on Industrial Electronics, Vol.40, No.3, 1993, p.355-363.
23. Ogata, K.: *Modern control engineering*. 1st ed., Pearson, Delhi 2016.
24. Korkmaz, M., Aydogdu, O., Dogan, H.: *Design and performance comparison of variable parameter nonlinear PID controller and genetic algorithm based PID controller*. 2012 International Symposium on Innovations in Intelligent Systems and Applications, 2012.
25. Guo, P., Wang, X., Han, Y.: *The enhanced genetic algorithms for the optimization design*. 3rd International Conference on Biomedical Engineering and Informatics, 2010, p. 2990-2994.